Identification of a random elastic medium by vibration tests

Christophe Desceliers, Christian Soize

IDENTIFICATION OF A RANDOM ELASTIC MEDIUM BY VIBRATION TESTS

C. Desceliers
University of Marne-la-vallée, Paris, France
christophe.desceliers@univ-mlv.fr

C. Soize
University of Marne-la-vallée, Paris, France
soize@univ-mlv.fr

Abstract. *This paper deals with the experimental identification of the probabilistic representation of a random field modeling the Young modulus of a non homogeneous isotropic elastic medium by experimental vibration tests. The random field representation is based on the polynomial chaos decomposition. The coefficients of the polynomial chaos are identified setting an inverse problem and then in solving an optimization problem related to the maximum likelihood principle.*

Keywords:*Random elastic medium, identification, polynomial chaos*

1. Introduction

For elastic random media, a fundamental question concerns the experimental identification of the probabilistic model of the elastic properties. In a recent work proposed by Desceliers, Ghanem and Soize (2004), this problem addressed : (1) A polynomial chaos representation of random fields to be identified is used. (2) An estimation of the coefficients of the chaos representation is performed by using the maximum likelihood method. (3) The experimental test is assumed to be static which generally requires a lot of experimental measurements for a very heterogeneous random medium. In this paper, we present an extension of this method in the context of experimental vibrational tests. The objective is (1) to use the mesurements of the response in a frequency band which allows the quality of the construction to be increased with respect to static measurements and (2) to have a method based on the use of vibrational tests instead of static tests.

2. Presentation of the method

The proposed method is presented through a simple example related to the experimental identification of the random field modeling the Young modulus of a random linear isotropic heterogeneous medium by vibrational tests. The data used for the identification correspond to experimental measurements of the frequency response functions related to the displacement field on the boundary of the specimen. In a first step, the proposed method consists in estimating the Young modulus field of each specimen. For this, the elastodynamic problem is written for the specimen and is discretized by the finite element method. The random Young modulus field is then projected on the finite element basis for which the random coefficients have to be identified. For each specimen the realization of the random coefficients are calculated by solving a first optimization problem allowing the norm between the measured and the calculated response functions of the specimen to be minimized. In a second step, these random coefficients whose realizations have been constructed, are then represented by using the polynomial chaos representation (see for instance Wiener, 1938, Ghanem and Spanos, 1991, Soize and Ghanem, 2003). In a last step, a second optimization problem allows the coefficients to be calculated by using the maximum likelihood method. Consequently, the probabilistic model of the random Young modulus field is completely defined.

3. Construction of an "experimental database" by Monte Carlo numerical simulation of the direct problem

In this paper, the «experimental database» is constructed by numerical simulation. The specimen is constituted of a non-homogeneous isotropic linear elastic medium occupying a three-dimensional bounded domain $\mathcal{D}$ with boundary $\partial\mathcal{D}$ given in a Cartesian system $Ox_1x_2x_3$. The geometry of domain $\mathcal{D}$ is a slender rectangular box shown in Fig. 1 whose dimensions along x_1, x_2 and x_3 are $L_1 = 1.3 \times 10^{-1}m$, $L_2 = 2 \times 10^{-2}m$ and $L_3 = 2 \times 10^{-2}m$. The structure is fixed on the part Γ_0 of $\partial\mathcal{D}$ for which the displacement field is zero.

The structure is subjected to an external point force denoted as $\mathbf{b}(t)$ and applied to the node A along x_1-axis (see Fig. 1). The Fourier transform $\widehat{\mathbf{b}}$ of $\mathbf{b}$ is the constant vector $(1, 0, 0)$ in the frequency band $[0, 50]$ kHz. The elastic medium is random. It is assumed that the Young modulus is random while the Poisson coefficient is deterministic. This assumption is introduced in order to simplify the presentation. The random Young modulus field is modeled by a positive-valued second-order random field $Y(\mathbf{x})$ defined by

$$Y(\mathbf{x}) = c_0\, g(c_1, c_2\, V(\mathbf{x})) \quad , \quad \forall \mathbf{x} \in \mathcal{D} \tag{1}$$

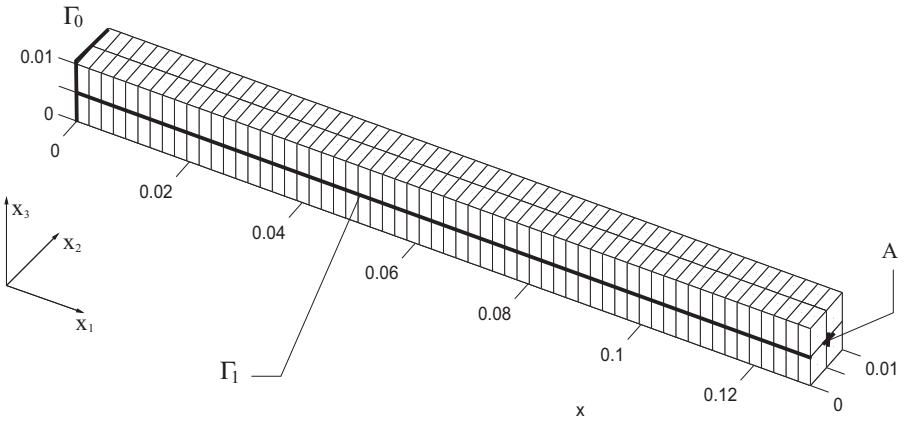

Figure 1. Definition of the specimen

in which $c_0 = 1.6663 \times 10^{10}\ N.m^{-2}$, $c_1 = 1.5625$ and $c_2 = 0.2$. The function $\theta \mapsto g(\alpha, \theta)$ from $\mathbb{R}$ into $]0\,, +\infty[$ is such that, for all θ in $\mathbb{R}$,

$$h(\alpha, \theta) = F^{-1}_{\Gamma_\alpha}(F_\Theta(\theta)) \quad ,$$

in which $\theta \mapsto F_\Theta(\theta) = P(\Theta \leq \theta)$ is the cumulative distribution function of the normalized Gaussian random variable Θ and where the function $p \mapsto F^{-1}_{\Gamma_\alpha}(p)$ from $]0\,, 1[$ into $]0\,, +\infty[$ is the reciprocal function of the cumulative distribution function $\gamma \mapsto F_{\Gamma_\alpha}(\gamma) = P(\Gamma_\alpha \leq \gamma))$ of the gamma random variable Γ_α with parameter α. In the right-hand side of Eq. (1) , $\{V(\mathbf{x}), \mathbf{x} \in \mathcal{D}\}$ is a second-order random field such that $E\{V(\mathbf{x})\} = 0$ and $E\{V(\mathbf{x})^2\} = 1$, defined by

$$V(\mathbf{x}) = \sum_{|\boldsymbol{\alpha}|=1}^{3} H_{\boldsymbol{\alpha}}(Z_1, Z_2, Z_3, Z_4)\, \sqrt{\gamma_{\boldsymbol{\alpha}}}\, \psi_{\boldsymbol{\alpha}}(\mathbf{x}/2) \quad , \tag{2}$$

in which $\{Z_1, Z_2, Z_3, Z_4\}$ are independent normalized Gaussian random variables, $\boldsymbol{\alpha}$ is a multi-index $(\alpha_1, \alpha_2, \alpha_3, \alpha_4) \in \mathbb{N}^4$, $|\boldsymbol{\alpha}| = \alpha_1 + \alpha_2 + \alpha_3 + \alpha_4$ and where $H_{\boldsymbol{\alpha}}(z_1, z_2, z_3, z_4) = H_{\alpha_1}(z_1) \times H_{\alpha_2}(z_2) \times H_{\alpha_3}(z_3) \times H_{\alpha_4}(z_4)$ in which $H_{\alpha_k}(z_k)$ is the normalized Hermite polynomial of order α_k such that

$$\int_{\mathbb{R}} H_{\alpha_k}(w)\, H_{\alpha_j}(w) \frac{1}{\sqrt{2\pi}} e^{-\frac{1}{2}w^2}\, dw = \delta_{\alpha_k \alpha_j}\ .$$

In the right-hand side of Eq. (2) , $\{\gamma_{\boldsymbol{\alpha}}\}_{1 \leq |\boldsymbol{\alpha}| \leq 3}$ and $\{\psi_{\boldsymbol{\alpha}}\}_{1 \leq |\boldsymbol{\alpha}| \leq 3}$ are defined as the eigenvalues and the eigeinfunctions of the the integral linear operator $\mathbf{C}$ defined by the kernel $C(\mathbf{x}, \mathbf{x}') = \exp(-|x_1 - x'_1|/L)$ in which $L = L_1/40$ and where $\mathbf{x} = (x_1, x_2, x_3)$ and $\mathbf{x}' = (x'_1, x'_2, x'_3)$ belong to $\mathcal{D}$. This means that the correlation length of the random field is much smaller than the length L_1 of the specimen. The eigenvalue problem related to operator $\mathbf{C}$ is then written as

$$\int_{\mathcal{D}} C(\mathbf{x}, \mathbf{x}') \psi_{\boldsymbol{\alpha}}(\mathbf{x}') d\mathbf{x}' = \gamma_{\boldsymbol{\alpha}}\, \psi_{\boldsymbol{\alpha}}(\mathbf{x}) \quad . \tag{3}$$

It should be noted that, $Y(\mathbf{x}) = Y(x_1)$ and consequently, $Y(\mathbf{x})$ is independent of x_2 and x_3. Figure 2 shows the mean value $\mathbf{x} \mapsto E\{Y(\mathbf{x})\}$ where $E\{\}$ denotes the mathematical expectation. Figure 3 shows the graph of the normalized autocorrelation function $(\mathbf{x}, \mathbf{x}') \mapsto E\{Y(\mathbf{x})Y(\mathbf{x}')\}/(E\{Y(\mathbf{x})\}\, E\{Y(\mathbf{x}')\})$. Finally, it is assumed that the Poisson coefficient $\mu = 0.3$ and the mass density $\rho = 2.7 \times 10^3\ Kg/m^3$ are deterministic real constants.

The finite element mesh of the structure is shown in Fig. 1 and consists of 8-node isoparametric 3D solid finite elements. There are $N_d = 1620$ degrees of freedom. Let $\mathbf{Z} = (Z_1, Z_2, Z_3, Z_4)$ be the $\mathbb{R}^4$-valued random variable constituted of the 4 independent random variables in Eq. (2) (the random germ of uncertainties). Let $[K(\mathbf{Z})]$ be the random stiffness matrix with values in the set of all the positive-definite symmetric $(N_d \times N_d)$ real matrices. Let $[M]$ and $[D]$ be the mass and the damping matrices such that $[D] = a\,[M]$ with $a = 10^3\ s^{-1}$. Matrices $[M]$ and $[D]$ are

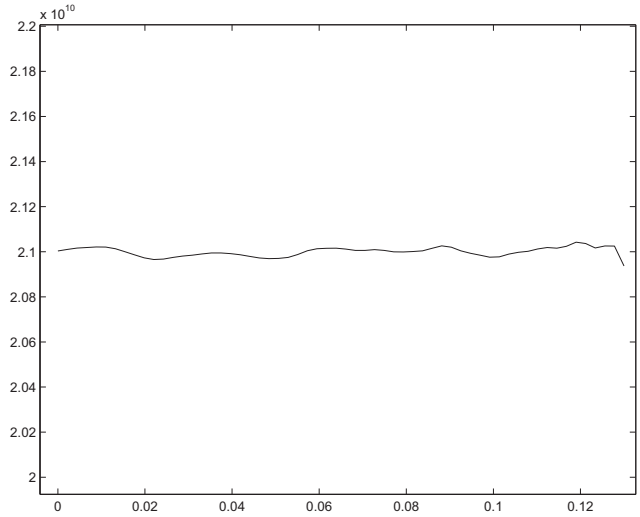

Figure 2. Graph of the function $\mathbf{x} \mapsto E\{Y(\mathbf{x})\}$ where $\mathbf{x} = (x_1, x_2, x_3)$ with $x_2 = x_3 = 0$. Horizontal axis: x_1. Vertical axis: $E\{Y(\mathbf{x})\}$.

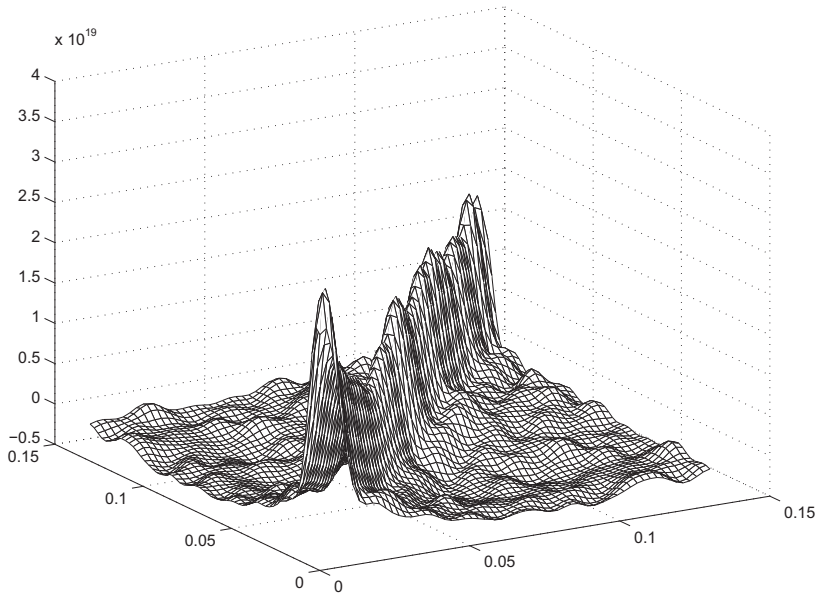

Figure 3. Graph of the function $(\mathbf{x}, \mathbf{x}') \mapsto E\{Y(\mathbf{x})Y(\mathbf{x}')\}/(E\{Y(\mathbf{x})\}\, E\{Y(\mathbf{x}')\})$ where $\mathbf{x} = (x_1, x_2, x_3)$ and $\mathbf{x}' = (x'_1, x'_2, x'_3)$ with $x_2 = x_3 = 0$ and $x'_2 = x'_3 = 0$. Horizontal axis: x_1 and x'_1. Vertical axis: $E\{Y(\mathbf{x})Y(\mathbf{x}')\}/(E\{Y(\mathbf{x})\}\, E\{Y(\mathbf{x}')\})$.

deterministic positive-definite symmetric $(N_d \times N_d)$ real matrices. The $\mathbb{R}^{N_d}$-valued random-frequency-response function $\omega \mapsto \mathbf{U}(\omega)$ related to the nodal displacements is such that

$$[A(\omega; \mathbf{Z})]\mathbf{U}(\omega) = \mathbf{f}(\omega) \quad ,$$

in which $[A(\omega; \mathbf{Z})] = -\omega^2 [M] + i\,\omega [D] + [K(\mathbf{Z})]$ is the dynamic stiffness matrix and where $\mathbf{f}(\omega)$ is the $\mathbb{R}^{\mathbb{N}_d}$-vector of the external forces. Let $\mathbf{U}_\Gamma(\omega)$ be the vector corresponding to the $N_b = 60$ nodes belonging to $\partial\mathcal{D}$ which can be written as $\mathbf{U}_\Gamma(\omega) = \mathbb{P}(\mathbf{U}(\omega))$ in which $\mathbb{P}$ is a linear mapping from $\mathbb{R}^{\mathbb{N}_d}$ into $\mathbb{R}^{\mathbb{N}_b}$. The experimental database is constituted of $m = 100$ realizations of random vector $\mathbf{U}_\Gamma(\omega)$ which are denoted by $\mathbf{u}^1_\Gamma(\omega) = \mathbf{U}_\Gamma(\omega, \theta_1), \ldots, \mathbf{u}^m_\Gamma(\omega) = \mathbf{U}_\Gamma(\omega, \theta_m)$ corresponding to the specimens and for ω running through the frequency band of analysis.

4. Identification of the random field modeling the Young modulus by solving an inverse problem

The finite element approximation $\widetilde{Y}$ of random field Y indexed by $\mathcal{D}$ is written as $\widetilde{Y}(\mathbf{x}) = \sum_{k=1}^{N} R_k h_k(x_1)$ in which $h_1(x_1), \ldots, h_N(x_1)$ are the usual linear interpolation functions related to the finite element mesh of domain $\mathcal{D}$, where $N = 60$ is the degree of this approximation and where $R_1, \ldots R_N$ are the random coefficients. We introduce the $\mathbb{R}^N$-valued random variable $\mathbf{R}$ such that $\mathbf{R} = (R_1, \ldots, R_N)$. Let $[\widetilde{A}(\omega; \mathbf{R})]$ be the random dynamical stiffness matrix constructed by using the finite element approximation $\widetilde{Y}(\mathbf{x})$ of the Young modulus. For each realization $\mathbf{u}_\Gamma^j(\omega)$ belonging to the experimental database, the realization $\mathbf{r}^j = \mathbf{R}(\theta_j)$ of the random variable $\mathbf{R}$ are constructed by solving the nonlinear optimization problem

$$\min_{\mathbf{r}^j} \ell_{dyn}(\mathbf{r}^j, \mathbf{u}_\Gamma^j) \quad , \tag{4}$$

in which

$$\ell_{dyn}(\mathbf{r}^j, \mathbf{u}_\Gamma^j) = \sum_{k=1}^{N_{band}} \int_{B_k} \left\| \mathbb{P}\left([\widetilde{A}(\omega; \mathbf{r}^j)]^{-1} \mathbf{f}(\omega) \right) - \mathbf{u}_\Gamma^j(\omega) \right\|^2 d\omega \quad . \tag{5}$$

In the right-hand side of Eq. (5) , $B_k = [\omega_{\min,k}, \omega_{\max,k}]$ with $\omega_{\min,k} = \omega_k - B_{eq,k}/2$ and $\omega_{\max,k} = \omega_k + B_{eq,k}/2$ where $B_{eq,k}$ is an equivalent bandwidth related to the eigenfrequency ω_k of the mean model of the specimens and where N_{band} is the number of bands considered for the identification. It should be noted that the optimization problem introduced (Desceliers, Ghanem and Soize, 2004) in order to solve the inverse problem to calculate the realizations $\mathbf{r}^1, \ldots, \mathbf{r}^m$ of random vector $\mathbf{R}$ is based on an elastostatic problem. In this case, the experimental database is constituted of static measurements and the optimisation problem is

$$\min_{\mathbf{r}^j} \ell_{stat}(\mathbf{r}^j, \mathbf{u}_\Gamma^j) \quad , \tag{6}$$

in which

$$\ell_{stat}(\mathbf{r}^j, \mathbf{u}_\Gamma^j) = \left\| \mathbb{P}\left([\widetilde{A}(0; \mathbf{r}^j)]^{-1} \mathbf{f}(0) \right) - \mathbf{u}_\Gamma^j(0) \right\|^2 \quad .$$

The optimization problems defined by Eqs. (4) and (6) are solved by using a least-squares estimation of nonlinear parameters (see, Marquardt, 1963). Finally, for all $\mathbf{x}$ fixed in $\mathcal{D}$, the realizations $\widetilde{y}^1(\mathbf{x}) = \widetilde{Y}(\mathbf{x}; \theta_1), \ldots, \widetilde{y}^m(\mathbf{x}) = \widetilde{Y}(\mathbf{x}; \theta_m)$ of random variable $\widetilde{Y}(\mathbf{x})$ are constructed by using the relation $\widetilde{y}^j(\mathbf{x}) = \mathbf{h}(x_1)^T \mathbf{r}^j$ in which $\mathbf{h}(x_1) = (h_1(x_1), \ldots, h_N(x_1))$. Figure 4 shows the graph of realization $x_1 \mapsto \widetilde{y}^1(\mathbf{x})$ with $x_2 = x_3 = 0$ constructed by solving Eq. (4) («dynamic inverse problem») and Eq. (6) («static inverse problem»). It can be seen that the dynamical inverse problem gives more accurate results than the static inverse problem. This can be explained by considering the dynamical inverse problem as the set of a large number of static inverse problems with different loading cases $\{\mathbf{f}(\omega), \omega \in \cup_{k=1}^{N_{band}} B_k\}$.

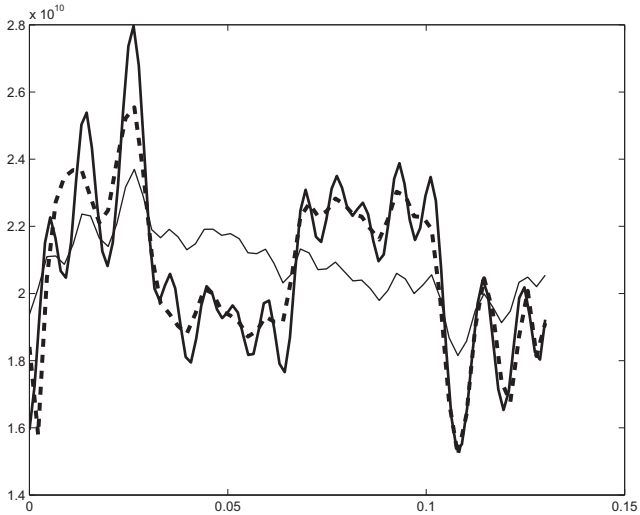

Figure 4. Graph of $x_1 \mapsto Y(\mathbf{x}; \theta_1)$ (thick solid line) and graph of realization $x_1 \mapsto \widetilde{y}^1(\mathbf{x})$ with $x_2 = x_3 = 0$ constructed by solving the «dynamic inverse problem» (dash line) with $N_{band} = 5$ and the «static inverse problem» (thin solid line). Horizontal axis: x_1. Vertical axis: $Y(\mathbf{x}; \theta_1)$ and $\widetilde{Y}^1(\mathbf{x})$

5. Statistical reduction

The size of the random vector $\mathbf{R}$ can be reduced. Let $\lambda_1 \geq \ldots \geq \lambda_N$ be the eigenvalues of the covariance matrix $[C_{\mathbf{R}}]$ of random vector $\mathbf{R}$. The normalized eigenvectors associated with the eigenvalues $\lambda_1, \ldots, \lambda_N$ are denoted by $\boldsymbol{\varphi}_1, \ldots, \boldsymbol{\varphi}_N$. Consequently, the random vector $\mathbf{R}$ can be written as

$$\mathbf{R} = \underline{\mathbf{R}} + \sum_{k=1}^{N} Q_k \sqrt{\lambda_k} \boldsymbol{\varphi}_k \quad ,$$

in which $Q_1, \ldots, Q_N$ are N centered real-valued random variables defined by $\sqrt{\lambda_k} Q_k = \boldsymbol{\varphi}_k^T (\mathbf{R} - \underline{\mathbf{R}})$ where $\underline{\mathbf{R}} = E\{\mathbf{R}\}$ such that for all k and ℓ, $E\{Q_k\} = 0$ and $E\{Q_k Q_\ell\} = \delta_{k\ell}$. Figure 5 displays the graph of the function $n \mapsto \sum_{k=1}^{n} \lambda_k^2$. It can be deduced that random vector $\mathbf{R}$ can be approximated by the random vector $\underline{\mathbf{R}} + [\Phi]\,[\Lambda]\mathbf{Q}^\mu$ with $\mu = 15 < N$ in which the $(\mu \times \mu)$ matrix $[\Lambda]$ and the $(N \times \mu)$ matrix $[\Phi]$ are such that $[\Lambda]_{\ell k} = \delta_{\ell k} \sqrt{\lambda_\ell}$ and $[\Phi]_{\ell k} = [\boldsymbol{\varphi}_k]_\ell$ and where $\mathbf{Q}^\mu = (Q_1, \ldots, Q_\mu)$. For all $j = 1, \ldots, m$, the realization $\mathbf{q}^j = \mathbf{Q}^\mu(\theta_j)$ of random vector $\mathbf{Q}^\mu$ is calculated by $\mathbf{q}^j = [\Lambda]^{-1}[\Phi]^T(\mathbf{r}^j - \underline{\mathbf{R}})$.

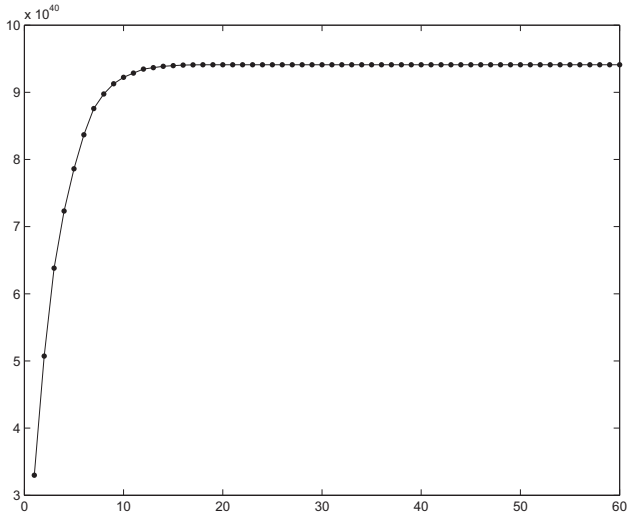

Figure 5. Convergence analysis of the statistical reduction : graph of function $n \mapsto \sum_{k=1}^{n} \lambda_k^2$. Horizontal axis n, vertical axis $\sum_{k=1}^{n} \lambda_k^2$.

6. Chaos decomposition

Let $\mathbf{W}^\nu = (W_1, \ldots, W_\nu)$ be the normalized Gaussian random vector such that $E\{W_i W_j\} = \delta_{ij}$. The truncated Chaos representation of the $\mathbb{R}^\mu$-valued random variable $\mathbf{Q}^\mu$ in terms of $\mathbf{W}^\nu$ is written as

$$\mathbf{Q}^{\mu,\nu} = \sum_{\boldsymbol{\alpha},|\boldsymbol{\alpha}|=1}^{+\infty} \mathbf{a}_{\boldsymbol{\alpha}} H_{\boldsymbol{\alpha}}(\mathbf{W}^\nu) \quad , \tag{7}$$

where $\boldsymbol{\alpha}$ is a multi-index belonging to $\mathbb{N}^\nu$ and where $H_{\boldsymbol{\alpha}}(\mathbf{W}^\nu)$ is the multi-indexed Hermite polynomials (see section 3). The coefficients $\mathbf{a}_{\boldsymbol{\alpha}}$ belonging to $\mathbb{R}^\mu$ are such that $\sum_{\boldsymbol{\alpha},|\boldsymbol{\alpha}|=1}^{+\infty} \mathbf{a}_{\boldsymbol{\alpha}} \mathbf{a}_{\boldsymbol{\alpha}}^T = [\,I_\mu]$ in which $[\,I_\mu]$ is the $(\mu \times \mu)$ unit matrix. The truncated Chaos representation of random vector $\mathbf{Q}^{\mu,\nu}$ is denoted by $\mathbf{Q}^{\mu,\nu,d}$ and is such that $\mathbf{Q}^{\mu,\nu,d} = \sum_{\boldsymbol{\alpha},|\boldsymbol{\alpha}|=1}^{d} \mathbf{a}_{\boldsymbol{\alpha}} H_{\boldsymbol{\alpha}}(\mathbf{W}^\nu)$. Consequently, for all $\mathbf{x} \in \mathcal{D}$, the random Young modulus $\widetilde{Y}(\mathbf{x})$ can be approximated by the random variable $\widetilde{Y}^{\mu,\nu,d}(\mathbf{x}) = \mathbf{h}(x_1)^T\,([\Phi]\,[\Lambda]\mathbf{Q}^{\mu,\nu,d} + \underline{\mathbf{R}})$.

The maximum likelihood method (see for instance Serfling, 1980) is used to estimate parameters $\mathbf{a}_{\boldsymbol{\alpha}}$ from realizations $\mathbf{q}^1, \ldots, \mathbf{q}^m$. We then have to solve the following problem of optizimation: find $\mathbb{A} = \{\mathbf{a}_{\boldsymbol{\alpha}}, |\boldsymbol{\alpha}| = 1, \ldots, d\}$ such that

$$\max_{\mathbb{A}} L(\mathbf{q}^1, \ldots, \mathbf{q}^m; \mathbb{A}) \quad , \quad \text{with} \quad \sum_{\boldsymbol{\alpha},|\boldsymbol{\alpha}|=1}^{d} \mathbf{a}_{\boldsymbol{\alpha}} \mathbf{a}_{\boldsymbol{\alpha}}^T = [\,I_\mu] \tag{8}$$

where $L(\mathbf{q}^1, \ldots, \mathbf{q}^m; \mathbb{A}) = p_{\mathbf{Q}^{\mu,\nu,d}}(\mathbf{q}^1, \mathbb{A}) \times \ldots \times p_{\mathbf{Q}^{\mu,\nu,d}}(\mathbf{q}^m, \mathbb{A})$ is the likelihood function associated with observations $\mathbf{q}^1, \ldots, \mathbf{q}^m$ and where $p_{\mathbf{Q}^{\mu,\nu,d}}$ is the probability density function of $\mathbf{Q}^{\mu,\nu,d}$. However, the optimization problem defined

by Eq. (8) yields a very high computational cost induced by the estimation of the joint probability density functions $p_{\mathbf{Q}^{\mu,\nu,d}}(\mathbf{q}^j, \mathbb{A})$ (even for reasonable values of the length μ of random vector $\mathbf{Q}^{\mu,\nu,d}$). Consequently, it is proposed to substitute the usual likelihood function by the pseudo-likelihood function

$$\widetilde{L}(\mathbf{q}^1, \ldots, \mathbf{q}^m; \mathbb{A}) = \prod_{k=1}^{\mu} p_{Q_k^{\mu,\nu,d}}(q_k^1, \mathbb{A}) \times \ldots \times \prod_{k=1}^{\mu} p_{Q_k^{\mu,\nu,d}}(q_k^m, \mathbb{A}) \tag{9}$$

where $\mathbf{q}^j = (q_1^j, \ldots, q_\mu^j)$ and $\mathbf{Q}^{\mu,\nu,d} = (Q_1^{\mu,\nu,d}, \ldots, Q_\mu^{\mu,\nu,d})$ and where $p_{Q_k^{\mu,\nu,d}}$ is the probability density function of random variable $Q_k^{\mu,\nu,d}$. Finally, the following problem of optimization is substituted to the problem defined by Eq. (8) . Find $\mathbb{A} = \{\mathbf{a}_{\boldsymbol{\alpha}}, |\boldsymbol{\alpha}| = 1, \ldots, d\}$ such that

$$\max_{\mathbb{A}} \widetilde{L}(\mathbf{q}^1, \ldots, \mathbf{q}^m; \mathbb{A}) \quad , \quad \text{with} \quad \sum_{\boldsymbol{\alpha}, |\boldsymbol{\alpha}|=1}^{d} \mathbf{a}_{\boldsymbol{\alpha}} \mathbf{a}_{\boldsymbol{\alpha}}^T = [\, I_\mu] \quad . \tag{10}$$

7. Convergence Analysis

In order to perform a convergence analysis of the method proposed in this paper, the normalized random variables $\mathcal{Y}(\mathbf{x})$ and $\widetilde{\mathcal{Y}}^{\mu,\nu,d}(\mathbf{x})$ defined by $\mathcal{Y}(\mathbf{x}) = Y(\mathbf{x})/E\{Y(\mathbf{x})\}$ and $\widetilde{\mathcal{Y}}^{\mu,\nu,d}(\mathbf{x}) = \widetilde{Y}^{\mu,\nu,d}(\mathbf{x})/E\{\widetilde{Y}^{\mu,\nu,d}(\mathbf{x})\}$, for all $\mathbf{x} \in \mathcal{D}$, are introduced. Figure 6 shows the graphs of functions $\mathbf{x} \mapsto E\{\mathcal{Y}(\mathbf{x})\mathcal{Y}(\mathbf{x}')\}$ (thick dashed line) and $\mathbf{x} \mapsto E\{\widetilde{\mathcal{Y}}^{\mu,\nu,d}(\mathbf{x})\widetilde{\mathcal{Y}}^{\mu,\nu,d}(\mathbf{x}')\}$ where $\mathbf{x} = (x_1, x_2, x_3)$ and $\mathbf{x}' = (x_1', x_2', x_3')$ with $x_2 = x_3 = 0$ and $x_2' = x_3' = 0$, for $x_1' = 0.0888$ and with $d = 5$, $\mu = 15$, $\nu = 2, 3$ (thin dashed lines) and $\nu = 4, 5, 6, 7, 8$ (thin solid lines). It can be seen that the probabilistic model is converged for $\nu = 4$. The remaining error is due to the truncating of the statistical reduction defined in Section 5.

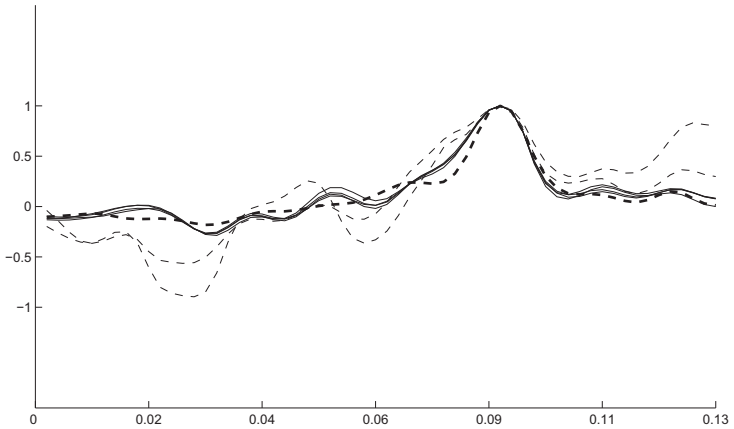

Figure 6. Graphs of functions $\mathbf{x} \mapsto E\{\mathcal{Y}(\mathbf{x})\mathcal{Y}(\mathbf{x}')\}$ (thick dashed line) and $\mathbf{x} \mapsto E\{\widetilde{\mathcal{Y}}^{\mu,\nu,d}(\mathbf{x})\widetilde{\mathcal{Y}}^{\mu,\nu,d}(\mathbf{x}')\}$ where $\mathbf{x} = (x_1, x_2, x_3)$ and $\mathbf{x}' = (x_1', x_2', x_3')$ with $x_1 = 0.0520$, $x_2 = x_3 = 0$ and $x_2' = x_3' = 0$ with $d = 5$, $\mu = 15$, $\nu = 2, 3$ (thin dashed lines) and $\nu = 4, 5, 6, 7$ (thin solid lines). Horizontal axis: x_1. Vertical axis: $E\{\mathcal{Y}(\mathbf{x})\mathcal{Y}(\mathbf{x}')\}$ and $E\{\widetilde{\mathcal{Y}}^{\mu,\nu,d}(\mathbf{x})\widetilde{\mathcal{Y}}^{\mu,\nu,d}(\mathbf{x}')\}$

8. Identification of the probabilistic model

Each Fig. 7 shows the graphs of $\mathbf{x} \mapsto E\{\mathcal{Y}(\mathbf{x})\mathcal{Y}(\mathbf{x}')\}$ (thick dashed line) and $\mathbf{x} \mapsto E\{\widetilde{\mathcal{Y}}^{\mu,\nu,d}(\mathbf{x})\widetilde{\mathcal{Y}}^{\mu,\nu,d}(\mathbf{x}')\}$ (thin solid line) where $\mathbf{x} = (x_1, x_2, x_3)$ and $\mathbf{x}' = (x_1', x_2', x_3')$ with $x_2 = x_3 = 0$ and $x_2' = x_3' = 0$, for $x_1' = 0.0173$ (Fig. 7a), $x_1' = 0.0520$ (Fig. 7b), $x_1' = 0.0888$ (Fig. 7c), $x_1' = 0.1105$ (Fig. 7d) and with $d = 5$, $\mu = 15$, $\nu = 4$.

For all $\mathbf{x} \in \mathcal{D}$, let $y \mapsto p_{\mathcal{Y}(\mathbf{x})}(y; \mathbf{x})$ and $y \mapsto p_{\widetilde{\mathcal{Y}}^{\mu,\nu,d}(\mathbf{x})}(y; \mathbf{x})$ be the probability density functions of the random variables $\mathcal{Y}(\mathbf{x})$ and $\widetilde{\mathcal{Y}}^{\mu,\nu,d}(\mathbf{x})$. Each Fig. 8 shows the graphs of $y \mapsto \log_{10}(p_{\mathcal{Y}(\mathbf{x})}(y; \mathbf{x}))$ (thick solid line) and $y \mapsto \log_{10}(p_{\widetilde{\mathcal{Y}}^{\mu,\nu,d}(\mathbf{x})}(y; \mathbf{x}))$ (thin solid line) where $\mathbf{x} = (x_1, x_2, x_3)$ with $x_2 = x_3 = 0$ and $x_1 = 0.0152$ (Fig. 8a), $x_1 = 0.1018$ (Fig. 8b) and with $d = 5$, $\mu = 15$ and $\nu = 4$. It can be seen that the probabily density function is accurately identified.

9. Conclusion

A method for solving the stochastic inverse problem using chaos representation of the stochastic field to be identified and an experimental database is proposed. This method extends the method proposed in (Desceliers, Ghanem and Soize,

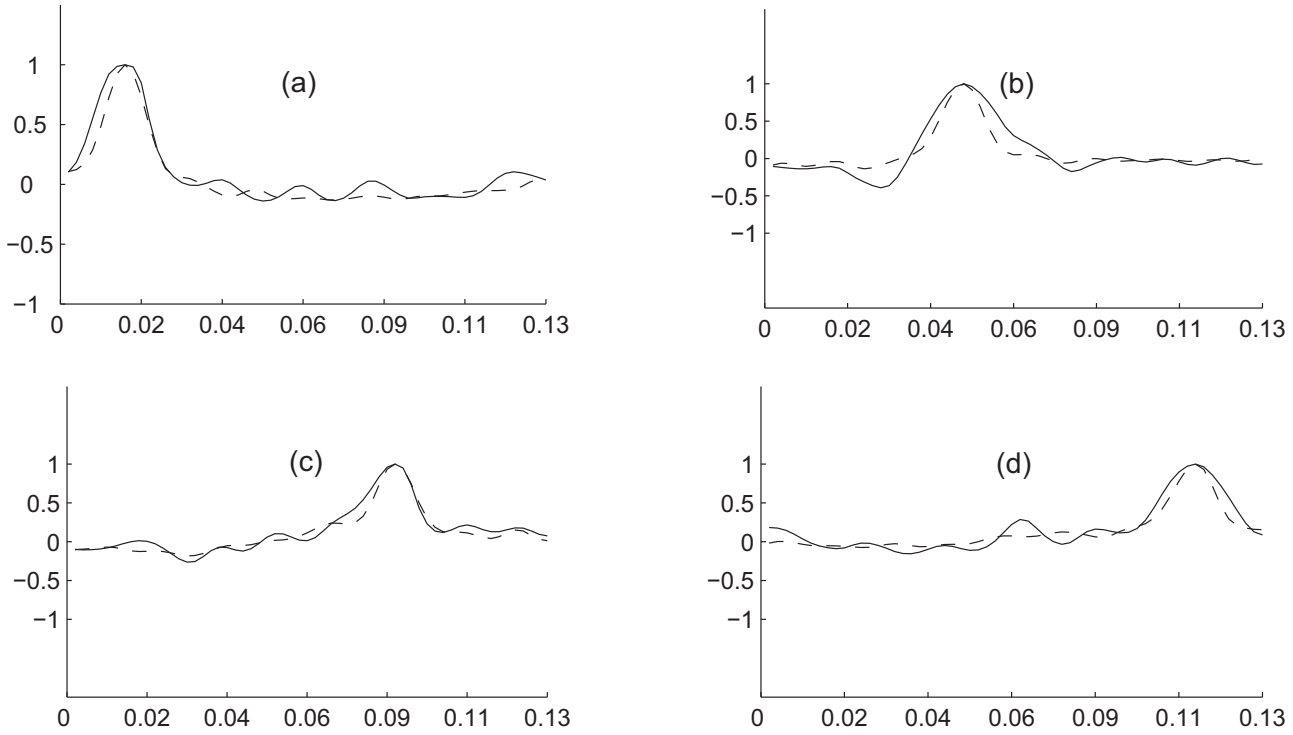

Figure 7. Graphs of $\mathbf{x} \mapsto E\{\mathcal{Y}(\mathbf{x})\mathcal{Y}(\mathbf{x}')\}$ (thick dashed line) and $\mathbf{x} \mapsto E\{\widetilde{\mathcal{Y}}^{\mu,\nu,d}(\mathbf{x})\widetilde{\mathcal{Y}}^{\mu,\nu,d}(\mathbf{x}')\}$ (thin solid line) where $\mathbf{x} = (x_1, x_2, x_3)$ and $\mathbf{x}' = (x_1', x_2', x_3')$ with $x_2 = x_3 = 0$ and $x_2' = x_3' = 0$, for $x_1' = 0.0173$ (Fig. 7a), $x_1' = 0.0520$ (Fig. 7b), $x_1' = 0.0888$ (Fig. 7c), $x_1' = 0.1105$ (Fig. 7d) and with $q = 5$, $\mu = 15$, $\nu = 4$. Horizontal axis: x_1. Vertical axis: $E\{\mathcal{Y}(\mathbf{x})\mathcal{Y}(\mathbf{x}')\}$ and $E\{\widetilde{\mathcal{Y}}^{\mu,\nu,d}(\mathbf{x})\widetilde{\mathcal{Y}}^{\mu,\nu,d}(\mathbf{x}')\}$

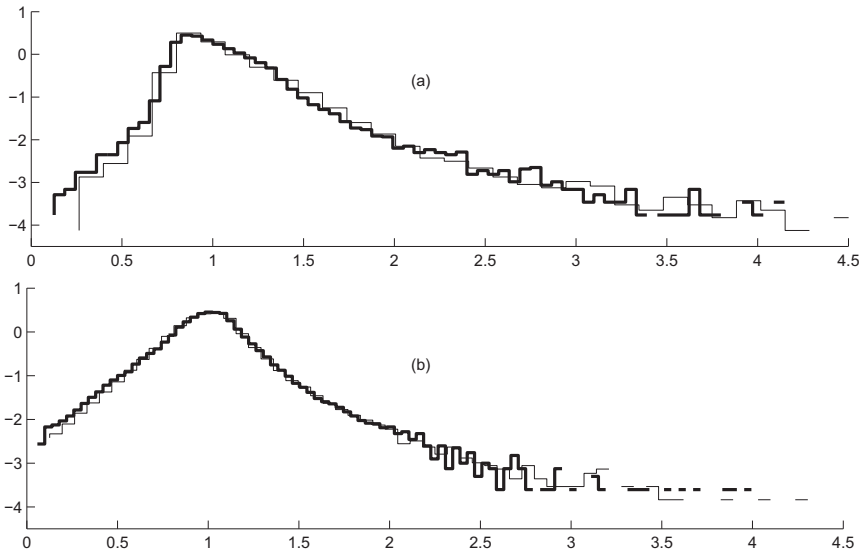

Figure 8. Graphs of $y \mapsto \log_{10}(p_{\mathcal{Y}(\mathbf{x})}(y;\mathbf{x}))$ (thick solid line) and $y \mapsto \log_{10}(p_{\widetilde{\mathcal{Y}}^{\mu,\nu,d}(\mathbf{x})}(y;\mathbf{x}))$ (thin solid line) where $\mathbf{x} = (x_1, x_2, x_3)$ with $x_2 = x_3 = 0$ and $x_1 = 0.0152$ (Fig. 8a), $x_1 = 0.1018$ (Fig. 8b) and with $d = 5$, $\mu = 15$ and $\nu = 4$. Horizontal axis: y. Vertical axis: $\log_{10}(p_{\mathcal{Y}(\mathbf{x})}(y;\mathbf{x}))$ and $\log_{10}(p_{\widetilde{\mathcal{Y}}^{\mu,\nu,d}(\mathbf{x})}(y;\mathbf{x}))$.

2004) to the case of experimental vibrational tests. The proposed method uses the maximum likelihood principle to identify the coefficients of the chaos representation. For presented example, this method allows any probabilistic quantities to be identified such as the autocorrelation function of the random field and the marginal probability density functions.

10. References

Desceliers, C., and Ghanem, R., and Soize, C., 2004, " Maximum Likelihood Estimation of Stochastic Chaos Representations from Experimental Data", (submitted to IJNME)

Wiener, N., 1938, "The Homogeneous Chaos" , American Journal of Mathematics, **60**: 897-936.

Ghanem, R., and Spanos, P., 1991, " Stochastic Finite Elements: A Spectral Approach", Springer-Verlag, New York.

Soize, C., and Ghanem, R., 2003, "Physical Systems with Random Uncertainties: Chaos Representations with Arbitrary Probability Measure",SIAM Journal of Scientific Computing. (in press)

Marquardt D., 1963, "An Algorithm for Least-squares Estimation of Nonlinear Parameters", SIAM Journal Applied Mathematics, **11**: 431-441

Serfling, R. J., 1980, "Approximation Theorems of Mathematical Statistics", John Wiley & Sons.